AIP | Journal of Applied Physics

Tailoring of crystal phase and Néel temperature of cobalt monoxides nanocrystals with synthetic approach conditions

A. V. Ravindra, B. C. Behera, P. Padhan, O. I. Lebedev, and W. Prellier

Citation: Journal of Applied Physics **116**, 033912 (2014); doi: 10.1063/1.4890512
View online: http://dx.doi.org/10.1063/1.4890512
View Table of Contents: http://scitation.aip.org/content/aip/journal/jap/116/3?ver=pdfcov
Published by the AIP Publishing

Tailoring of crystal phase and Néel temperature of cobalt monoxides nanocrystals with synthetic approach conditions

A. V. Ravindra,[1] B. C. Behera,[1] P. Padhan,[1] O. I. Lebedev,[2] and W. Prellier[2]
[1]*Department of Physics, Indian Institute of Technology Madras, Chennai 600036, India*
[2]*Laboratoire CRISMAT, CNRS UMR 6508, ENSICAEN, 6 Bd du Marechal Juin, F-14050 Caen Cedex, France*

(Received 9 May 2014; accepted 6 July 2014; published online 17 July 2014)

Cobalt monoxide (CoO) nanocrystals were synthesized by thermal decomposition of cobalt oleate precursor in a high boiling point organic solvent 1-octadecene. The X-ray diffraction pattern and transmission electron microscopy studies suggest that pure face-centered-cubic (fcc) phase of CoO can be synthesized in the temperature range of 569–575 K. Thermolysis product at higher synthesis temperature 585 K is a mixture of fcc and hexagonal-closed-packed (hcp) phases. These nanocrystals are single crystals of CoO and exhibit mixture of two types of morphologies; one is nearly spherical with 5–25 nm diameter, and other one is 5–10 nm thick flake. The pure fcc-CoO nanocrystals show enhanced, and mixture of fcc- and hcp-CoO nanocrystals show reduced antiferromagnetic ordering temperature. Such results provide new opportunities for optimizing and enhancing the properties and performance of cobalt oxide nanomaterials. © *2014 AIP Publishing LLC*. [http://dx.doi.org/10.1063/1.4890512]

In 1961, Néel suggested that at nanometer scale the antiferromagnetic (AFM) cobalt monoxide (CoO) should exhibit superparamagnetism or weak ferromagnetism.[1] He attributed the permanent magnetic moment to an uncompensated number of spins on two sublattices. Indeed, anomalous magnetic properties in the nanostructures of AFM have been observed, which are interpreted by several mechanisms such as (i) a size effect which substantially lowers the Néel point,[2] (ii) the appearance of uncompensated spins on the particle surface,[3] (iii) the creation of a spin-glass structure,[4] (iv) the formation of the complicated magnetic structure caused by the canting of the spins and increasing number of magnetic sublattices,[5] and (v) the existence of the random magnetic disorder caused by other factors such as enhanced grain surface effect[6] and magnetically disordered shell.[7] Thus, the possibility of observing non-intrinsic property of CoO nanostructures in its magnetization is very high. On the other hand, a variety of Raman spectra have been observed in the CoO nanostructures[8–10] due to the transformation of crystal structure of the CoO with the Raman excitation laser power. This transformation of CoO phase is found to be very localized. Therefore, the consequences of the laser power lead to an ambiguity in the assignment of the Raman bands of CoO.[11,12]

The CoO generally crystallizes into one of the following two phases: stable rock-salt phase with space group $Fm\bar{3}m$ and less stable wurtzite phase with space group $P6_3mc$, in which Co^{2+} is octahedrally and tetrahedrally coordinated, respectively.[13] The face-centered-cubic (fcc) CoO structure holds a thermodynamically stable state, but the hexagonal-closed-packed (hcp) structure is relatively unstable and can be easily transformed into a cubic structure by applying heat and/or pressure due to the preference of Co^{2+} for octahedral coordination.[14] Theoretical lattice energy calculations suggest that the rock-salt structure is more stable than the wurtzite structure by 0.27 eV per CoO, when the sum of the ionic cohesive energy and the octahedral site preference energy for both the phases are compared.[15] Despite the numerous reports on synthesis of CoO, the synthesis of pure CoO at nano-scale is found to be rather difficult and limited, as it is often being contaminated with more stable Co_3O_4 or Co metal phases. In this article, we report the synthesis of single crystal CoO nanocrystals by thermal decomposition of cobalt oleate precursor in a high boiling point solvent 1-octadecene with different synthesis temperatures. The phase, morphology, Néel temperature, and magnetization of these CoO nanocrystals strongly depend on the synthesis temperature.

The synthesis of cobalt monoxide nanocrystals was carried out using commercially available reagents. All the chemicals, including absolute ethanol, hexane, oleic acid, 1-octadecene $(90+\%)$, sodium oleate $(C_{18}H_{33}O_2Na;\ 85+\%)$, and $CoCl_2.6H_2O$ $(97+\%)$, were purchased from Sigma Aldrich. All the chemicals were used as-received without any further purification. The cobalt oleate complex was prepared by reaction of sodium oleate and Co^{2+} chloride. The details of experimental procedure has been described previously.[12] Cobalt monoxide nanocrystals are synthesized from the mixture of 3.68 g of cobalt oleate complex, 40 ml of 1-octadecene, and 2 ml of oleic acid at 569, 575, and 585 K synthesis temperatures. The reaction mixture was refluxed/aged at these temperatures for 1 h under N_2 flow with continuous stirring using magnetic stirrer. Then, the reaction mixture was cooled down to room temperature and transferred to a 15 ml centrifuge tube together with a 20 ml mixture of ethanol and hexane, with a volume ratio of 1:3. The de-emulsified mixture was then centrifuged at 6500 rpm for 15 min to isolate the supernatant liquid. The synthesis product was then dispersed in hexane for storage.

The crystallinity and phase composition of the thermolysis products were examined using Philips X'pert Pro X-ray diffractometer. The shape, size, and chemical composition of the nanocrystals were analyzed by Field Emission Scanning Electron Microscope (FESEM) Quanta 400 F and transmission electron microscopy (TEM) coupled with high-resolution TEM (HRTEM) using Tecnay G2 30 UT

microscope operated at 300 kV and having 0.17 nm point resolution. The Raman spectra were recorded on a Jobin-Yvon LabRAM HR800UV spectrometer. The magnetization (M) measurements were carried out using a superconducting quantum interference device based magnetometer (Quantum Design MPMS-5).

All these reactions were thermodynamically controlled with reaction pathways plausible from the starting materials except for different synthesis temperatures. The X-ray diffraction patterns of thermolysis products synthesized at different temperatures are shown in Fig. 1. These X-ray profiles show strong diffraction peaks that can be indexed to the pure *hcp* and *fcc* cobalt monoxide phases without any evidence of other phases. The peak position and relative intensity of all diffraction peaks for the two products (curves (a) and (b), in Fig. 1) match well with standard powder diffraction data. The X-ray diffraction reveals that the reaction mixture refluxed at temperatures 569 and 575 K has yielded fcc-CoO nanocrystals with lattice parameter 4.251 Å. On the other hand, the curve (c) of Fig. 1 indicates that the thermolysis product synthesized at temperature 585 K contains the mixture of both *hcp* and *fcc* cobalt monoxide phases. The average lattice parameter calculated from the X-ray pattern of the fcc-CoO nanocrystals synthesized at temperature 585 K was found to be 4.243 Å, which is closer to that of the pure fcc-CoO nanocrystals synthesized at temperatures 569 and 575 K and bulk CoO 4.26 Å.[13] We have also calculated the average lattice parameters of hcp-CoO phase of the mixture. The observed lattice parameters $a = b = 3.22$ Å and $c = 5.15$ Å are also in good agreement with that of the reported for bulk.[13]

The FESEM images of cobalt monoxide nanocrystals, shown in Fig. 2, indicate weak agglomeration of nanocrystals though they are well dispersed in hexane. From these images, we observed that the nanocrystals of all the samples show two types of morphologies; one is nearly spherical with 5 to 25 nm diameter and other is 5 to 10 nm thick flake. The nearly spherical morphology is predominant in the case

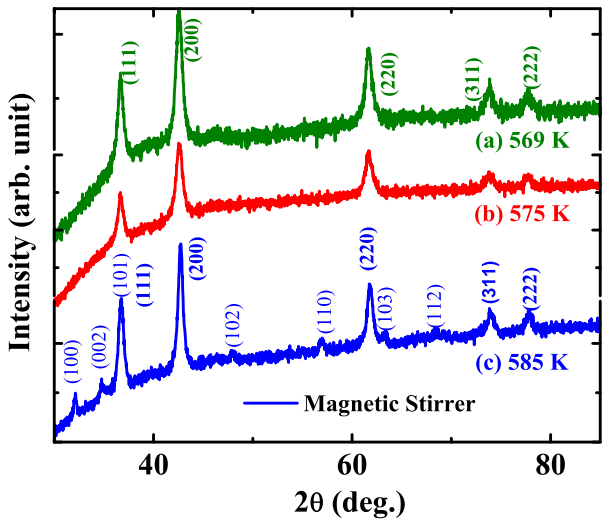

FIG. 1. The θ-2θ X-ray diffraction patterns of CoO nanocrystals synthesized at different temperatures. The peaks indexed with bold face (hkl) denote fcc phase of CoO while the peaks indexed with normal (hkl) represents hcp-CoO.

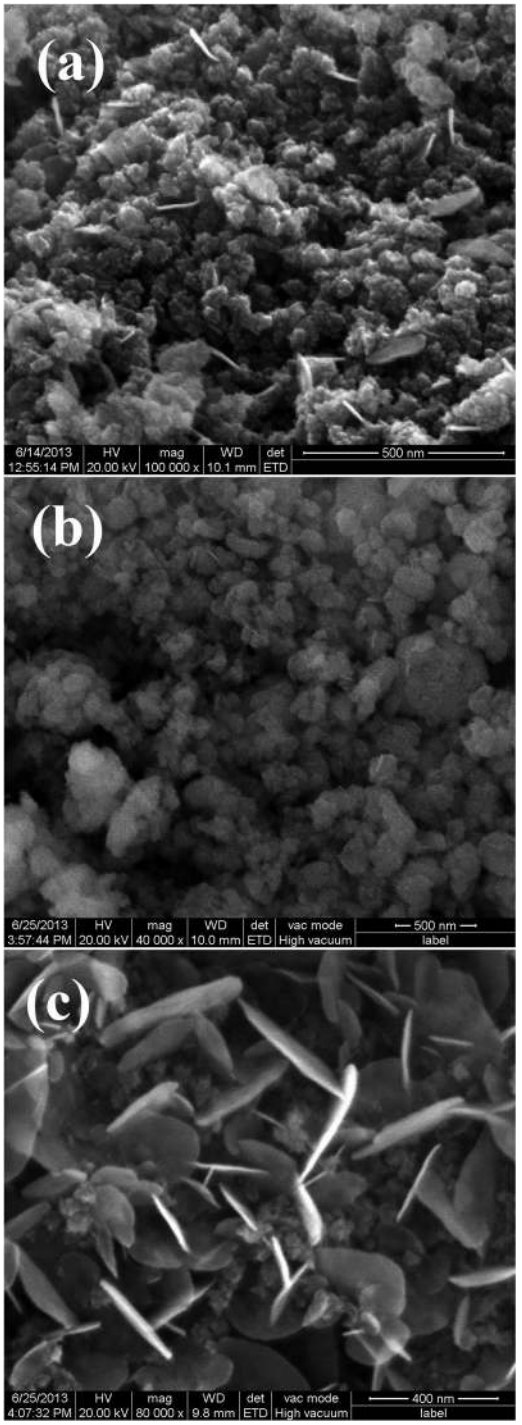

FIG. 2. High magnification FESEM images of CoO nanocrystals prepared at (a) 569 K, (b) 575 K, and (c) 585 K.

of nanocrystals with pure fcc-CoO (see Figs. 2(a) and 2(b)). More comprehensive information of the phase composition of CoO nanocrystals can be obtained from TEM studies. Set of the low magnification and HRTEM images together with corresponding electron diffraction (ED) patterns are shown in Fig. 3. It can be seen from the inset of Figs. 3(a) and 3(c) that the selected-area electron diffraction (SAED) pattern recorded from randomly distributed nanocrystals exhibits diffraction rings that correspond to only fcc-CoO. While, the SAED pattern in the inset of Fig. 3(e) clearly shows the

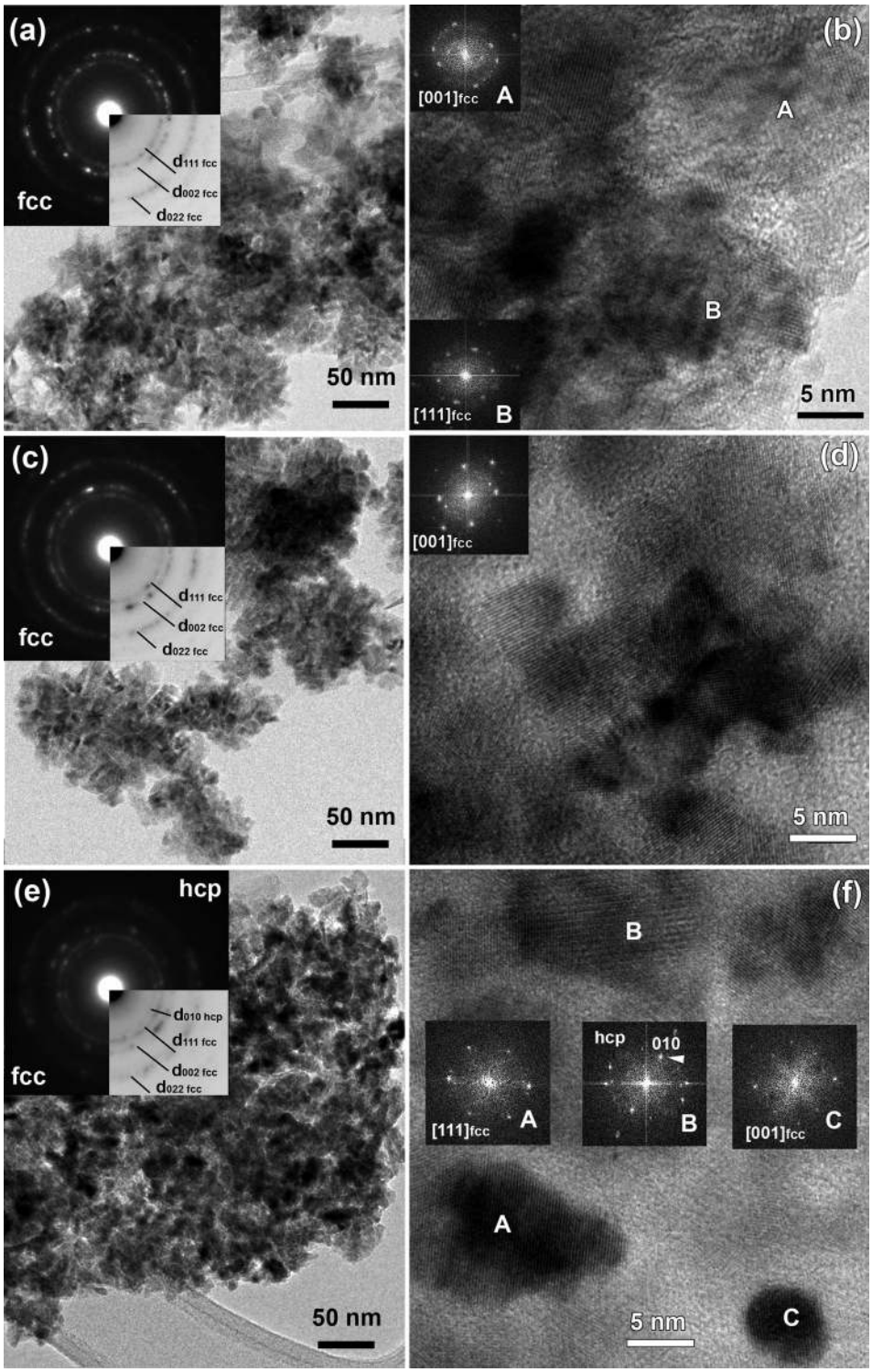

FIG. 3. Bright field TEM images and corresponding ED patterns of CoO samples prepared at (a) 569 K, (c) 575 K, and (e) 585 K. HRTEM images of CoO nanocrystals prepared at (b) 569 K, (d) 575 K, and (f) 585 K. FFT patterns taken from different HRTEM images of nanocrystals are given as inset.

diffraction rings match with two phases of CoO (fcc and hcp). Systematic HRTEM images indicated that all the nanocrystals are single crystals. Applying Fast Fourier Transform (FFT) to the HRTEM images of single nanocrystals allows us to identify their crystal phase. The nanocrystals marked as "A" and "B" in the HRTEM image (Fig. 3(b)) of the nanostructure synthesized at 569 K were processed by using the FFT and corresponding FFT patterns are shown in the insets of Fig. 3(b). The FFT patterns clearly indicate fcc-CoO nanocrystals imaged along [001] and [111] zone axis, which is consistent with the observed ring SAED pattern (Fig. 3(a)) and X-ray diffraction pattern of the nanocrystals. The similar situation is observed for sample prepared at 575 K (Figs. 3(c) and 3(d)) where only fcc-CoO phase has been observed. TEM results obtained from sample prepared at 585 K are shown in Figs. 3(e) and 3(f). In contrast to previous two samples, ED ring patterns can be indexed as mixture of fcc and hcp structures. Weak ring corresponding to 2.78 Å d-spacing is a clear indication of the presence of hcp phase and can be indexed to d_{010} lattice planes. The FFT patterns obtained

from different nanocrystals imaged in Fig. 3(f) (A, B, and C) are in agreement with ED patterns showing that nanocrystals marked as A and C are definitely fcc structure viewed along [111] and [001] zone axis while nanocrystal B exhibits d-spacing corresponding to hcp CoO phase. This data show further evidence of the observed X-ray pattern in Fig. 1.

The CoO nanocrystals are further studied using Raman scattering. Since the Co^{2+} ions are octahedrally coordinated to six O^{2-} ions in fcc-CoO, the O_h symmetry should lead to the observation of at least three Raman active modes (A_{1g}, E_g, and T_{2g}) at room temperature.[16,17] On the other hand, the Co^{2+} ions are tetrahedrally coordinated in hcp-CoO which belongs to the space group $P6_3mc$ with two formula units in the primitive cell and the zone-center optical phonons symmetry should lead to the observation of polar Raman active modes (A_1 and E_1) and nonpolar Raman active mode (E_2). However, a variety of Raman spectra have been observed on CoO and such variation of CoO Raman spectra is due to the gradual modification of CoO structure by the excitation laser intensity of the Raman spectrometer.[11,12] Therefore, we have recorded the Raman spectra of all CoO nanocrystals with lowest possible excitation laser intensity (1 mW). The Raman spectra of the CoO nanocrystals synthesized at 569, 575, and 585 K are plotted in the Fig. 4. The Raman spectrum of fcc-CoO nanocrystals synthesized at 569 K shows a weak shoulder at 489 cm^{-1} and two prominent peaks at 540 and 690 cm^{-1} identified as E_g, T_{2g}, and A_{1g} modes, respectively.[12] Qualitatively, similar Raman spectrum is also observed for the CoO nanocrystals synthesized at higher temperatures. A red shift of E_g, T_{2g}, and A_{1g} modes is observed for nanocrystal synthesized at 575 K and of T_{2g} and A_{1g} modes for nanocrystal synthesized at 585 K. The Raman spectrum of nanocrystals synthesized at 585 K does not show any contribution from hcp-CoO structure that could be due to its relatively unstable structural state and can be easily transformed into a cubic structure by applying heat, laser power, and pressure.[14]

In Fig. 5, we show 5 G field-cooled (FC) temperature dependent magnetization M(T) of the CoO nanocrystals

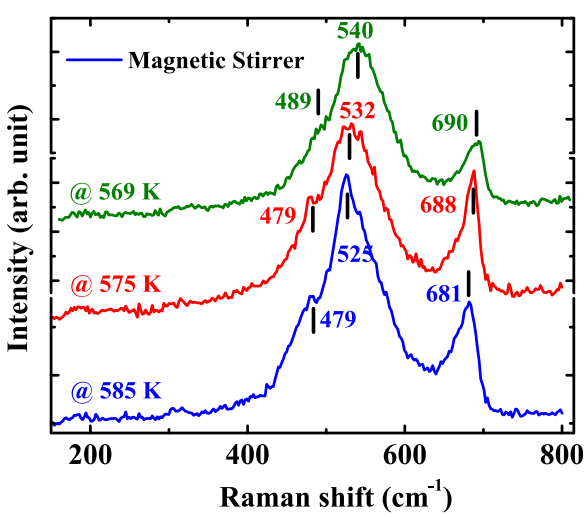

FIG. 4. Room temperature Raman spectra of CoO nanocrystals synthesized at (a) 569 K, (b) 575 K, and (c) 585 K.

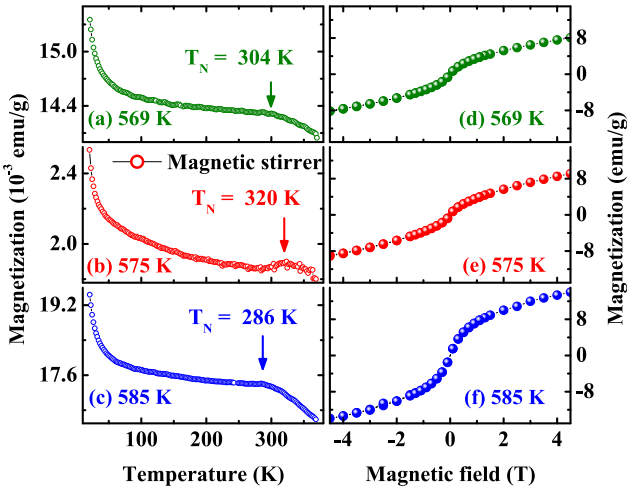

FIG. 5. Temperature [panel (a)–(c)] and magnetic field [panel (d)–(f)] dependent magnetization of CoO nanocrystals synthesized at temperatures 569, 575, and 585 K, respectively.

synthesized at 569, 575, and 585 K. In Fig. 5(a), the magnetization of the CoO nanocrystals synthesized at 569 K decreases rapidly and then slowly with the increase of temperature until an anomaly in magnetization is reached at 304 K. On further heating the nanocrystals upto 360 K, the magnetization deceases gradually. The temperature associated with the magnetic anomaly is identified as the Néel temperature (T_N) of the CoO. Interestingly, as the cooling field is increased to 100 G, the magnetic anomaly at ~304 K of the CoO nanocrystals disappear, which indicates weak antiferromagnetic nature of the nanocrystals. The M(T) of CoO nanocrystals synthesized at 575 K exhibits a peak at ~320 K, which is associated to the T_N. However, as the synthesis temperature is further increased to 585 K, the T_N of the CoO nanocrystals decreases to ~286 K. So, the CoO nanocrystals synthesized at 569 and 575 K exhibit enhanced T_N while the nanocrystals synthesized at 585 K shows reduced T_N compared to that of the bulk CoO ($T_N \sim 293$ K (Ref. 18)). In addition, the magnetization at temperature below T_N is superimposed to a larger paramagnetic signal due to the magnetic exchange coupling between the nanocrystals.[19]

The field dependent magnetization M(H) at 10 K of CoO nanocrystals synthesized at different temperatures is shown in the Fig. 5. In Fig. 5(d), as the magnetic field decreases from 4.5 T, the magnetization of the CoO nanocrystals synthesized at 569 K decreases linearly upto 0.15 T followed by nonlinear decrease till −0.15 T. On further decreasing the field to −4.5 T, the magnetization decreases linearly. Interestingly, the same path of magnetization is retraced when the magnetic field increases from −4.5 T to 4.5 T. Qualitatively similar M(H) curves with larger magnetization is observed for the CoO nanocrystals synthesized at higher temperatures, shown in Figs. 5(e) and 5(f). The maximum observed magnetization at 10 K under 4.5 T magnetic field corresponds to 8.07, 9.12, and 14.0 emu/g for the CoO synthesized at temperature 569, 575, and 585 K, respectively. In CoO, a saturation magnetization of 224 emu/g results if all Co spins in bulk CoO were to order ferromagnetically with a spin only moment of 3 μ_B.[20] Though the CoO nanocrystal

prepared at 585 K exhibits a large magnetization (14 emu/g), it is evident that the observed value of magnetization is significantly lower than that of the theoretically expected value of 224 emu/g for CoO with Co spin order ferromagnetically. So, a small ferromagnetically ordering of around 6% would thus follow for the CoO nanocrystal prepared at 585 K. However, this calculation does not consider the exchange coupling between the nanocrystals. But the presence of exchange coupling between the nanocrystals and/or surface disorder is clearly observed in the M(T); the increase of magnetization below Néel temperature. Therefore, the observed moments of these nanocrystals which are around 6% ferromagnetically order Co spin of CoO are attributed to the uncompensated surface spin[3,21] and paramagnetic exchange between the nanocrystals.[19] Hence, the nonlinear change of M(H) could be due to an appreciable net magnetic moment from uncompensated surface spins.[3,21]

In conclusion, single crystal nanocrystals of CoO prepared from the thermal decomposition of cobalt oleate at 569 and 575 K exhibit pure fcc-CoO phase. But further increase in the decomposition temperature to 585 K leads to the mixture of fcc and hcp-CoO phases. All CoO nanocrystals are single crystalline and exhibit mixture of two types of morphologies; one is nearly spherical with 5 to 25 nm diameter and other is 5 to 10 nm thick flake. These nanocrystals show red shift of Raman modes and enhanced magnetization at 10 K with increase of thermal decomposition temperature. The fcc-CoO shows enhanced, and mixture of fcc- and hcp-CoO shows reduced antiferromagnetic ordering temperature. Around 6% ferromagnetically order Co spin of CoO and the nonlinear change of M(H) of the CoO nanocrystals can be explained by the paramagnetic exchange between the nanocrystals and appreciable net magnetic moment from uncompensated surface spins.

We greatly acknowledge the financial support of New Faculty Seed Grant of IITM, LAFICS and the IFPCAR/CEFIPRA (Project No. 3908-1).

[1]L. Néel, Compt. Rend. **252**, 4075 (1961).
[2]V. Markovich, I. Fita, A. Wisniewski, D. Mogilyansky, R. Puzniak, L. Titelman, C. Martin, and G. Gorodetsky, Phys. Rev. B **81**, 094428 (2010).
[3]H. T. Zhang and X. H. Chen, Nanotechnology **16**, 2288 (2005).
[4]J. Nogués, J. Sort, V. Langlais, V. Skumryev, S. Suriñach, J. S. Muñoz, and M. D. Baró, Phys. Rep. **422**, 65 (2005).
[5]R. H. Kodama, S. A. Makhlouf, and A. E. Berkowitz, Phys. Rev. Lett. **79**, 1393 (1997).
[6]P. Dey, T. K. Nath, and A. Banerjee, Appl. Phys. Lett. **91**, 012504 (2007).
[7]N. J. O. Silva, A. Millan, F. Palacio, M. Martins, T. Trindade, I. Puente-Orench, and J. Campo, Phys. Rev. B **82**, 094433 (2010).
[8]C. A. Melendres and S. Xu, J. Electrochem. Soc. **131**, 2239 (1984).
[9]M. M. Vuurman, D. J. Stufkens, Ad. Oskam, G. Deo, and I. E. Wachs, J. Chem. Soc., Faraday Trans. **92**, 3259 (1996).
[10]H. C. Choi, Y. M. Jung, I. Noda, and S. B. Kim, J. Phys. Chem. B **107**, 5806 (2003).
[11]K. An, N. Lee, J. Park, S. C. Kim, Y. Hwang, J.-G. Park, J.-Y. Kim, J.-H. Park, M. J. Han, J. Yu, and T. Hyeon, J. Am. Chem. Soc. **128**, 9753 (2006).
[12]A. V. Ravindra, B. C. Behera, and P. Padhan, J. Nanosci. Nanotechnol. **14**, 5591 (2014).
[13]W. S. Seo, J. H. Shim, S. J. Oh, E. K. Lee, N. H. Hur, and J. T. Park, J. Am. Chem. Soc. **127**, 6188 (2005).
[14]J. R. Singer, Phys. Rev. **104**, 929 (1956).
[15]R. W. Grimes and K. P. D. Lagerlof, J. Am. Ceram. Soc. **74**, 270 (1991).
[16]K. Nakamoto, in *Infrared and Raman Spectra of Inorganic and Coordination Compounds Part A: Theory and Applications in Inorganic Chemistry* (Wiley, New York, 1997), p. 384.
[17]D. Gallant, M. Pezolet, and S. Simard, J. Phys. Chem. B **110**, 6871 (2006).
[18]J. B. Tracy, D. N. Weiss, D. P. Dinega, and M. G. Bawendi, Phys. Rev. B **72**, 064404 (2005).
[19]L. Zhang, D. Xue, and C. Gao, J. Magn. Magn. Mater. **267**, 111 (2003).
[20]D. P. Dutta, G. Sharma, P. K. Manna, A. K. Tyagi, and S. M. Yusuf, Nanotechnology **19**, 245609 (2008).
[21]L. Néel, in *Low Temperature Physics*, edited by C. Dewitt, B. Dreyfus, and P. D. de Gennes (Gordon and Beach, New York, 1962), p. 413.